Publishing House
AKAPIT

COMPUTER METHODS IN MATERIALS SCIENCE

Informatyka w Technologii Materiałów

Vol. 13, 2013, No. 2

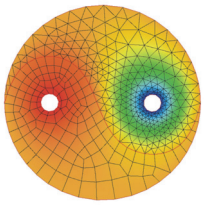

INVESTIGATION OF THE HEAT TRANSPORT DURING THE HOLLOW SPHERES PRODUCTION FROM THE TIN MELT

MICHAEL PETROV[1,2], PAVEL PETROV[2], JUERGEN BAST[1], ANATOLY SHEYPAK[3]

[1] Technical University Mining Academy of Freiberg, Institute of Machine Elements, Design and Manufacturing, Leipzigerstr. 30, 09596 Freiberg, Germany
[2] Moscow State University of Mechanical Engineering (MAMI), Department „Car Body Making and Metal Forming", B. Semenovskaya street 38, 107023 Moscow, Russia
[3] Moscow State Industrial University (MSIU), Department „Electrical, Heating and Hydraulic Engineering and Energy machines", Avtozavodskaya street 16, 115280 Moscow, Russia
**Corresponding author: petroffma@gmail.com*

Abstract

The present paper reveals one of the energy efficient ways of the units (hollow spheres) production for cellular structures for their further application in light weight constructions, realized through the metallurgical procedure. The metallurgical method exhibit all known methods in intelligence, because it based on the own physical properties of the used materials and boundary conditions of the process, not involving any organically core and preparation of the powder and slurries. These small hollow spheres made from different materials could change the weight of a construction part essentially, used as acoustic and thermal insulation and also as protection against vibrations. They can be used as a unit cell for big parts and alone filled with an inert gas, e.g. fusion targets. Pure tin shells were produced intransient (thixotropic) state of materials by elevated temperatures (close to the melting point of the pure tin) and several simulation steps were used, to determine the preferable boundary conditions. To one of them belongs the investigation of the temperature fields during the formation process. The heat transport from the tin melt into the semi-solid tin shell influence the nucleation process so the solid wall should be formed before the gas starts to form the inner hollow space. Otherwise the semi-solid shell will be broken by the gas pressure or the inner hollow space does not occur. For these purposes the CFD- (Computational Fluid Dynamic) and FEM-commercial codes such as FLUENT and Solid Works Simulation Package respectively were taken. At the end the data verification of the obtained simulation results with the measurements on the laboratory stand and theoretical calculations were carried out. Current investigation was completed by the determination of the whole temperature fields on the side surface of the form nozzle, which was obtained from a thermogram captured with the help of an infrared camera (IRC).

Key words: hollow spheres, spherical shells, tin melt, FEM, CFD, Solid Works, Fluent, thermography, heat transport

1. INTRODUCTION

Generally any production route consists of one or several production, treatment and controlling operations which are connected together through automation devices. For hollow spheres production the metallurgical technique, illustrated in figure 1, was used because of its high effectiveness and low production costs. The property of the product changes through the microstructure development results from the thermal energy consumption during the primary crystallization and further heat treatment under different regimes. The main controlling operations can be also implemented to obtain the spheres outer geometry, strength/ductility and inner geometry. Once the products were sorted the structure as-

ISSN 1641-8581

sembling occurs depending on the application cases. The current paper is focused on the first two steps in this line (metal melting and hollow sphere/shell solidification).

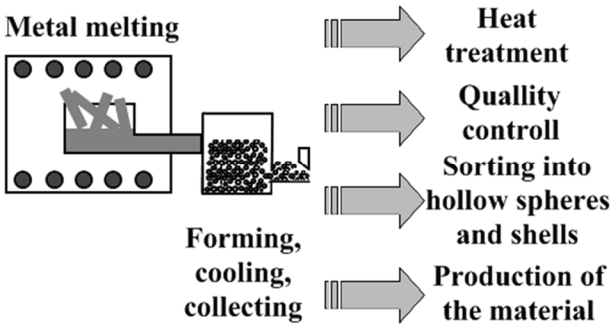

Fig. 1. *General process route of hollow spheres/shells production.*

2. EXPERIMENTAL EQUIPMENT

Designed and manufactured labor stand for metal hollow spheres and shells production from the tin melt was investigated. The melting, dosing and controlling of the solidification process occur in a special heating unit, which was made in a „sandwich" like assembly from copper and aluminum plates, tempered by heating rods. It allows adjusting the temperature in a narrow range and performing the nozzle tempering with a high precision.

The whole metal melting process runs in three stages: 1) preparing the metallic melt (optionally: alloying, degassing, protecting gas against oxidization procedure); 2) switch on the heating devices (furnace, heating unit); 3) process initiation: forming gas is fed to the tin melt through the gas needle and forms the spherical shells at the nozzle. Further description of the equipment could be found elsewhere (Petrov & Bast, 2010; Petrov, 2012).

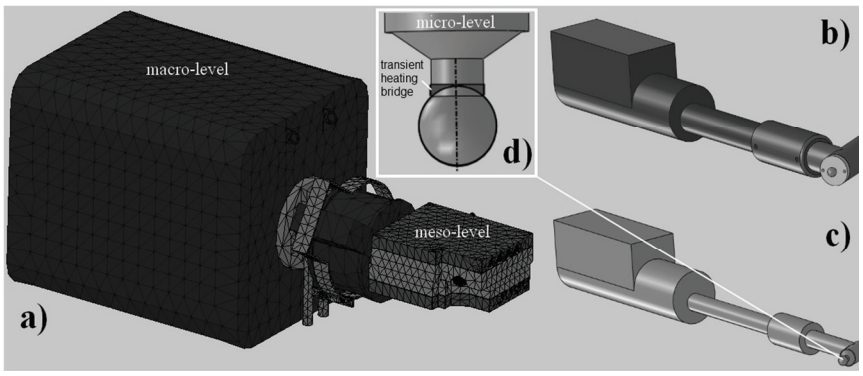

Fig. 2. *Prepared model for simulation (a), model of the crucible (b) with the tin melt volume(c) and hollow sphere of 3 mm in diameter and the wall thickness of 0,5 mm (d).*

3. NUMERICAL SIMULATION

Although the similar production technique was discussed by Kendall (1981), Dorogotowcev & Merkulyev (1989) several differences and resulted setups of the heat transport problems were not still numerical investigated. Also many fundamental aspects on the heat transport given by e.g. Baehr & Stephan (2006) should to be coupled to the manufacturing route and equipment.

3.1. Model preparation

To perform the numerical simulation the CAD-models of heating devices inclusive crucible were optimized before meshing (fasteners connections were closed, sharply corners were rounded and the fiber thermal insulation was proposed as a material with homogeneous properties). To obtain adequate results different size of the mesh elements were applied: the biggest of 0,9 mm for the nozzle and 22,2 mm for the heating furnace with the common side ratio of volume tetraeder elements of 1,5. The simulated hollow sphere has a transient heating bridge, which connected the sphere with the main tin melt volume in the nozzle area as it is shown in figure 2d. It is expected that an additional heat amount will transferred into the spherical shell. It was assumed that the heating bridge elevates the temperature in the spherical shell, but the temperature difference stays the same. The lifetime of the bridge corresponds to the formation time of a single shell.

3.2. Temperature distribution in the system

During the simulation setup of the temperature distribution in the whole system (furnace – heating plates – nozzle) three main heat transport mechanisms (thermal conductivity, convection and radiation) were activated. To enable the simulation the following boundary conditions were assigned and are presented in the table 1. The simulation results delivered a homogeneous temperature distribution in the crucible, shown in figure 3.

Table 1. *Boundary conditions in the simulated system.*

Element	Heat source
Furnace	initial temperature on the refractory lining
Heating plates	initial temperature on each heating rod or capacity per rod
Inductor	initial temperature on the refractory lining

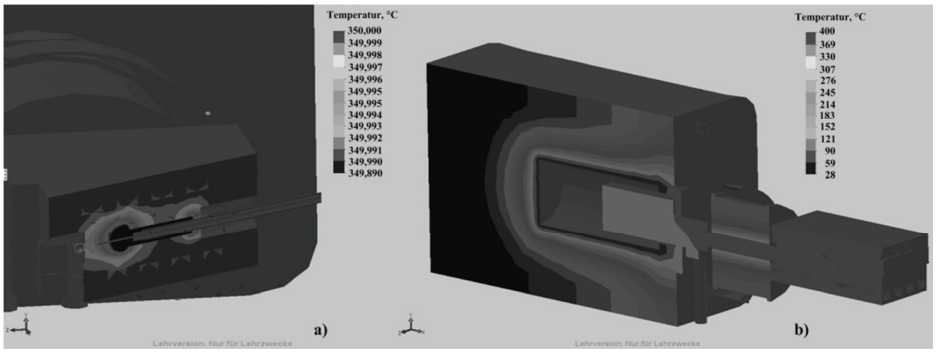

Fig. 3. *Temperature fields in the longitudinal cross section of the nozzle (a) and heating equipment (b).*

3.3. Temperature distribution in the heating plates (mesolevel)

The simulation of the heat transfer between the fluids and inside the heating system was investigated and represents the mesolevel of the system. The goal was to determine the expected temperature fields on the microlevel, i.e. at the nozzle. The heating unit is a „sandwich" like assembly and consists of an upper and lower blocks, produced from pure copper and cast aluminum alloy. In the aluminum upper and lower blocks the gravure of the nozzle was milled. After that the plates were mounted together. Because of the fact, that this heating unit will be placed in the space with a variable environmental temperature, the temperature distribution in the plates was calculated theoretically, after that compared with the simulation results and validated with the help of IRC, according the route in figure 4.

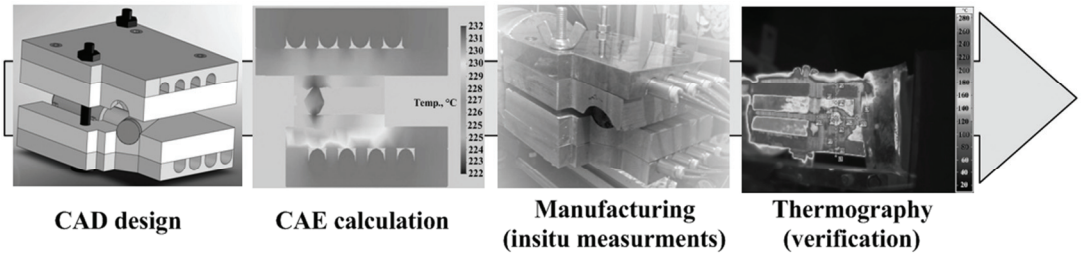

Fig. 4. *Construction stages of the heating plates.*

Theoretical calculation was based on the total capacity of the heating rods. The equation (1) connects the volume and thermal material properties of the plates (Petrov, 2012).

$$P = \frac{m_{Cu} \times c_{Cu} \times \Delta\vartheta}{t} + \frac{m_{Al} \times c_{Al} \times \Delta\vartheta}{t}, \quad (1)$$

where c_{Cu} and c_{Al} – specific heat capacity of copper and cast aluminum alloy; $\Delta\vartheta$ – temperature difference; m_{Cu} and m_{Al} – mass of the copper and aluminium plates.

From this analysis it was stated, that the thermal resistance (temperature drop or heat loss) due to plates stacks and heat loss due to convection and a little amount of the radiation does not exceed 5%.

To perform the simulation the mesh parameters were defined as follows: volume tetraeder elements, the biggest element of 10,2 mm, side ratio of 1,5. As a merit of the numerical simulation accuracy the duration of the heating stage was taken. The results from the transient heat transport simulation were compared with the temperature on the heating rod, placed in the upper copper plate, obtained with the help of thermocouple Ni-CrNi (type K). Giving the heat energy from the heating rods to the colder parts the main amount of it riches the nozzle. It was stated, that the amount of the transported heat energy is constant through a period of time and enough to guarantee the forming process discontinuity. At the same time the capacity of the heating rods determine also the heating time. Several in situ measurements were carried out to justify the proper choice of the boundary conditions. So the additional heat transfer mechanism, namely convection reduce the calculation error (compared to the measured value from the table 2) up to 8,4%.

Table 2. *Heating time, obtained for different simulation cases*

Heating stage, °C	Time, min : sec		Boundary conditions
	Experiment	Simulation	
from 0 up to 257	16:55	14:30	TR, HR + HC + T
		15:30	TR, HR + HC + T + C

where TR – transient heating process, HR – heat radiation, HC – heat capacity, T – constant temperature, C – convection.

Measurements with IRC has shown, that the temperature difference between the heating plates and the melt at the nozzle orifice stays by 16°C, during the simulation and theoretical investigations followed to a temperature of 16 – 25°C and 13 – 24°C respectively, where the greater value corresponds the greater heat loss in the system.

3.4. Temperature distribution at the nozzle (microlevel)

An obtained temperature distribution for mesolevel could be applied also for a microlevel. Because of a new fluid phase (forming gas) the new problem had to be defined. The temperature can be influenced by the forming gas expansion due to the differences of the cross sections of the pipeline and the feeding needle. The rash temperature drops of millisecond duration results strong tin melt undercooling. This undesirable effect leads to the process discontinuity due to metal solidification between two periods of hollow spheres formation. Through the simulation it could be shown, that even the test chamber temperature of 232°C (melting point of the pure tin) by investigated gas flow rates of an average value of 750 liter per hour does not allow to eliminate the undercooling effect on the displacement of 1,5 mm from the needle top of the nozzle presented in figure 5a.

Moreover once the temperature influence was cleared, the gas distribution in the tin melt was still unknown. To carry out the case study a special CFD-simulation and simple verification test were developed. The principle of the test is the periodic gas injection (frequency of 1 Hz) into the tin melt and measurement of the height of the invader cone zone. The aim of the test is to find out the cone height from the simulation results which corresponds to the real cone height from the verification test under the same boundary conditions and for the same time point, showed in figure 5b and 5c. The theoretical problem description can be found by Bohl (1991), Loycyanskiy (2003), Sheypak (2006) and other fundamentalists.

Because of the fact that the forming gas expands into the certain melt volume the expected temperature in the cross section could be calculated from the equation (2) as:

$$T_{o,th} = T_i \left(\frac{p_o}{p_i} \right)^{\frac{\chi-1}{\chi}}, \qquad (2)$$

where $\chi = \frac{c_p}{c_V}$ – isentropen exponent, $c_{p(v)}$ – isobare (isochore) specific heat capacity and $\frac{p_o}{p_i}$ – critical pressure ratio (p_o – pressure value after gas expansion and p_i – pressure value in the pipeline); T– temperature (index „i“ for inside, „o“ for outside and „th“ for theoretical)

The true temperature due to gas expansion was calculated from the equation (3), under the assumption, that the gas velocity exceeds the value of the velocity coefficient, defined as $\varphi = \sqrt{1-\xi'}$ with ξ' as a drag coefficient, and together with the energy equation:

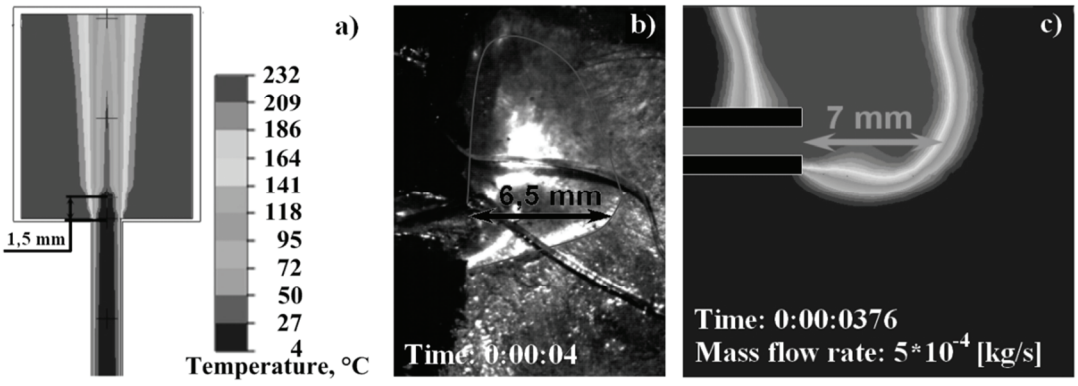

Fig. 5. *Phase and temperature distribution during the forming gas injection (a – numerical simulation of the temperature distribution after the gas expansion in the hot chamber, obtained in Solid Works; b – gas distribution in the tin melt, obtained with high speed camera, 100 fps;c – simulation of the gas distribution in the tin melt, obtained in FLUENT).*

$$T_o = T_i - \varphi^2 \left(T_i - T_{o,th}\right), \qquad (3)$$

So for an environmental temperature (ET) of 17°C the temperature differences stay by 7°C for experiment and 6°C for numerical simulation. Taking the height of the involved cone from the figure 5b of 6,5 mm on the diagram temperature-distance, shown in figure 6a, two areas can be pointed out: up to the distance of 6,5 mm and over this value. The expected temperature drop up to 6 – 7°C by initial ET of 17°C gives the distance of 5,5 mm from the nozzle. For an initial ET of 232°C the same distance will give the temperature decrease up to 45°C. The area above the distance of 6,5 mm is out of the gas distribution zone and not intended into the investigation.

figure 6c as thinner walls in figure 6b. Self the line for the thin wall has a greater slope as the line for the thick wall that means that the temperature gradient for thin walls under the same boundary conditions should be greater to transport the heat amount from the melt to activate the solidification process.

$$T_{th} = T(r) = T_i - \left(T_i - T_o\right) \frac{1 - \frac{r_i}{r}}{1 - \frac{r_i}{r_o}}, \qquad (4)$$

where T – temperature (index „i" for inner sphere surface, „o" for outer sphere surface and „th" for theoretical); r – arbitrary radius of the sphere.

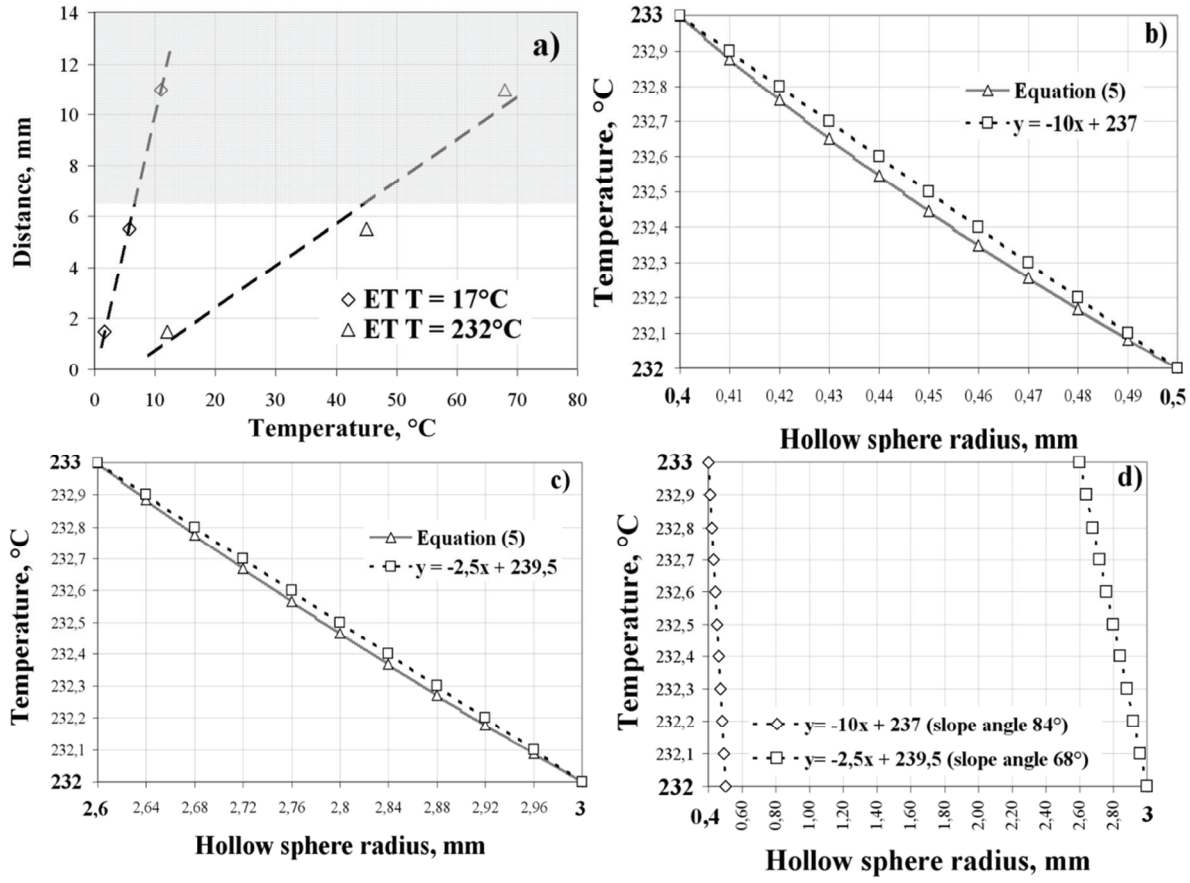

Fig. 6. *Temperature fields: temperature – distance diagram for determining undercooling effect (a); temperature distribution in the shell's wall with different radius and thickness (b and c) and slope of the linear temperature distribution curves (d).*

3.5. Temperature distribution in the sphere's wall (microlevel)

The temperature distribution in the spherical shell occurs also in micro level of the investigated system and can be calculated on hand the simple equation (4) with sphere radius as argument. Following the equation (4) the thicker walls propose the smaller temperature derivation from the linearity in

The hollow spheres in figure 7 were previously meshed with volume tetraeders' elements with the biggest size of 1 mm and side ratio of 1,5. After the simulation the obtained temperatures from the middle radius of the shell were compared with the calculated from the equation (4).

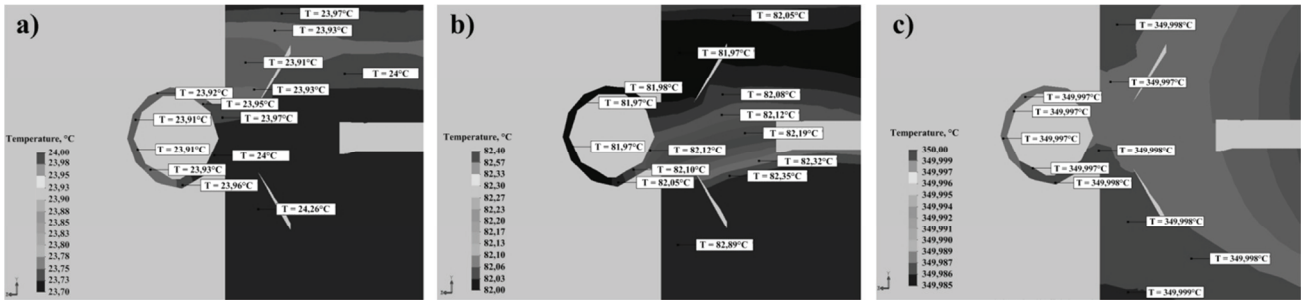

Fig. 7. Simulation of the temperature fields in the spherical shell at the time point of 20 seconds (a), 200 seconds (b), 2000 seconds (c).

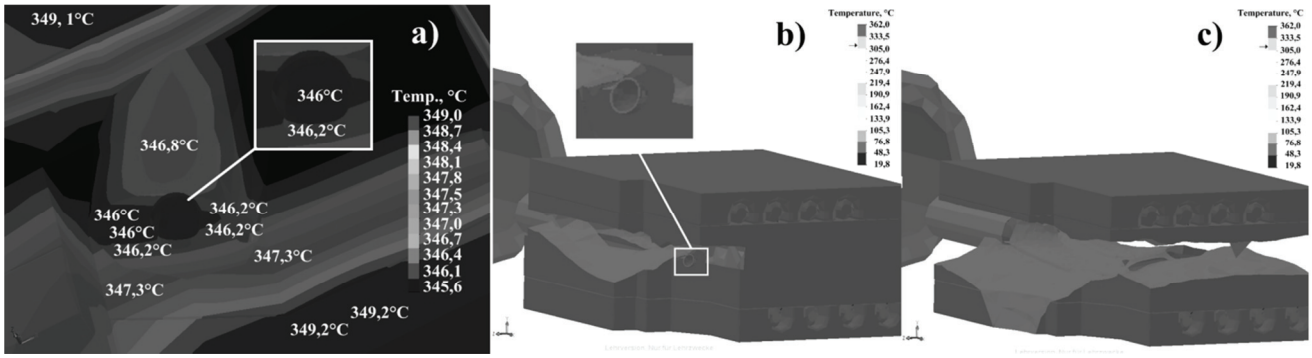

Fig. 8. Temperature fields on the outer surface of the spherical shell in 1000 seconds (a); ISO-surfaces in 900 seconds of calculation time for a temperature distribution from 313°C and higher (b) and from 314°C and higher (c).

3.6. Solidification process

From the simulation results presented in figure 8 it is clearly seen, that the solidification front moves from the top of the spherical shell to the nozzle orifice and the temperature difference does not exceed 0,2°C.

ISO-surfaces also show, that at the same time point the temperature in the spherical shell distributes very fast, differ from the temperatures on the other surfaces not more than on 1°C, presented in figures 8b and 8c.

The necessary solidification rate (*SR*) of a solidification process can be calculated from the equation (5):

$$SR = \frac{\Delta \vartheta}{t_{cal}}, \tag{5}$$

where t_{cal} – calculation time; $\Delta\vartheta$ – temperature difference on the outer and inner surfaces of the hollow sphere.

From the balance of heat fluxes described by Gottstein (2004) the heat of solidification can be obtained on the base of the equation (6):

$$\lambda_C \left(\frac{dT}{dx}\right)_C - \lambda_L \left(\frac{dT}{dx}\right)_L = h_S \left(\frac{dx}{dt_c}\right), \tag{6}$$

where T – temperature, h_S – heat of solidification; λ_C and λ_L – thermal conductivity of the crystal and melt respectively; x – distance (wall thickness), t_C – time of the crystal growth.

4. CONCLUSIONS AND OUTLOOKS

In the present paper the heat transport during the hollow spheres production from the tin melt was investigated in the numerical, theoretical and experimental way. The results go back on the micro-, meso- and macrolevel numerical problems of the investigated system, represented by simulation of the temperature distribution in heating system, heating plates and nozzle. Hollow spheres/shells could be produced directly from the tin melt if the boundary conditions were properly defined. The temperature fields in the sphere's wall due to small dimension of the sphere changes very quickly and need to be investigated separately with finer finite elements, because the temperature changes here during the whole processing time does not exceed 0,2°C. From the figures 6b and 6c the importance of the wall thickness in the heat transport problem is obtained. For thinner walls the temperature distribution shows greater deviation from a linear characteristic as for thicker walls, there temperature could be better described by a linear function. From the equation (4) follows, that non-uniform wall thickness of the shell

will cause different temperatures. Consequently the cooling rate will differ and the microstructure development in the wall will vary. Also the optical surface quality of the produced microsphere varies between rough for small cooling rates and smooth shiny for greater cooling rates.

Also a problem of undercooling effect due to expansion of not preheated forming gas at the nozzle was formulated and investigated. The prediction of the undercooling can be made on the hand of temperature-distance diagram in figure 6a and calculated from the equation (5) and (6). Both the information about the temperature distribution in the metallic melt and the gas distribution were used by the design and construction of the nozzle: nozzle placing, orifice diameter, temperature fields around the nozzle etc. These essential parts of the work make possible to increase the production capacity of the laboratory equipment.

The minimal diameter could be obtained from the Young-Laplace equation for hollow microspheres up to 1 mm in diameter and for bigger microspheres up to 3 – 4 mm in diameter the technique given by Petrov (2012) can be applied. The results can be used by the further microstructure prediction by function with two arguments, namely the outer shell diameter and wall thickness.

Acknowledgement. This paper was prepared in scope of the state contract № 16.740.11.0744, funded by Ministry of Education and Science of the Russian Federation.

REFERENCES

Baehr, H. D., Stephan, K., 2006, *Wärme- und Stoffübertragung*, 5th edition, Springer Verlag, Berlin, Heidelberg, New York (in German).

Bohl, W., 1991, *Technische Strömungslehre*, 9th edition, Vogel Buchverlag, Würzburg (in German).

Dorogotowcev, W., Merkulyev, J., 1989, *The methods of the hollow microspheres production*, Physical Lebedev Institute Publishing, Moscow (in Russian).

Gottstein, G., 2004, *Physical foundations of materials science*, Springer Verlag, Berlin, Heidelberg, New York.

Kendall, J.M., 1981, Hydrodynamic performance of an annular liquid jet: production of spherical shells, *Proceedings of the second international colloquium on drops and bubbles*, eds, LeCroisette, D. H., NASA JPL, Pasadena, 79-87.

Loycyanskiy, L.G., 2003, *Mechanic of fluids and gases*, 7th edition, Moscow (in Russian)

Petrov, M., Bast, J., 2010, Entwicklung einer Anlage zur Hohlkugelherstellung, Scientific reports on resource issues, *Proceedings of the 61. BHT (Berg- und Hüttenmännische Tagung)*, eds, Drebenstedt, C., TU Bergakademie Freiberg, Freiberg, Volume 3, 343-350 (in German).

Petrov, M., 2012, *Untersuchungen zur Hohlkugel- und Schalenherstellung direkt aus der metallischen Schmelze zu ihrer Anwendung in Leichtbaukomponenten*, PhD thesis, Freiberg (in German).

Sheypak, A.A., 2006, *Hydraulic and hydraulic drive systems*, 5th edition, MSIU Publishing, Moscow (in Russian).

ZAGADNIENIE TRANSPORTU CIEPŁA PODCZAS PRODUKCJI PUSTYCH KUL Z CYNY

Streszczenie

Praca przedstawia jedną z energooszczędnych metod produkcji zespołów struktur komórkowych (pustych kul) stosowanych w lekkich konstrukcjach. Opisany proces metalurgiczny produkcji kul wykorzystuje fizyczne własności zastosowanych materiałów oraz warunki brzegowe procesu bez wprowadzania proszków czy zawiesin. Puste kulki o małych średnicach wykonane z różnych materiałów mogą znacząco zmniejszyć wagę elementów konstrukcyjnych wykorzystywanych jako izolatory akustyczne i termiczne, a także jako ochrona przed wibracjami. Można je stosować jako komórki jednostkowe dla większych elementów lub jako elementy samodzielne wypełnione gazem obojętnym. Powłoki z czystej cyny produkowane są w temperaturze bliskiej temperatury topnienia materiału (w stanie tiksotropowym). W ramach pracy wykonano szereg symulacji komputerowych, które umożliwiły określenie właściwych warunków brzegowych procesu produkcji. Badano między innymi rozkład temperatury podczas procesu produkcji. Transport ciepła w procesie formowania powłok z cyny od stanu płynnego do stanu pół-stałego ma wpływ na proces zarodkowania, dlatego ścianki będące w stanie stałym powinny być formowane zanim gaz rozpocznie kształtowanie wnętrza powłoki. W przeciwnym wypadku pół-stała powłoka pęknie pod wpływem ciśnienia gazu lub w ogóle nie powstanie. W pracy do symulacji wykorzystano komercyjne programy FLUENT oraz pakiet SolidWorks. Wyniki symulacji zostały porównane z wynikami doświadczeń oraz obliczeń teoretycznych. Ponadto badania uzupełniono o wyznaczenie pola temperatury na powierzchni dyszy formującej dzięki termogramowi zarejestrowanemu kamerą na podczerwień (IRC).

Received: September 20, 2012
Received in a revised form: November 4, 2012
Accepted: November 21, 2012